CONF-8909210--7

DE90 008410

Bremsstrahlung Induced by 50 MeV H^0 Bombardment

C. Stein, K.W. Habiger, and B.R. Smith
Weapons Laboratory
Kirtland AFB, New Mexico 87117-6008

and

Oakley H. Crawford and R.H. Ritchie
Health and Safety Research Division
Oak Ridge National Laboratory
Oak Ridge, TN 37831

ABSTRACT

Three different thicknesses of aluminum targets, 0.0025 cm, 0.025 cm, and 0.32 cm were irradiated with 50-MeV neutral hydrogen atoms and the resultant bremsstrahlung radiation measured. The experimental results are compared with calculations that include bremsstrahlung by the projectile's electron and its cascade, bremsstrahlung by the cascade electrons that are generated by the projectile nucleus and quasifree-electron bremsstrahlung. The theoretical and experimental values of the total yield agree within a factor of three for all target thicknesses and all bremsstrahlung energies.

Bremsstrahlung Induced by 50 MeV H^o Atom Bombardment

I. Introduction

The continuum of x rays induced by ion bombardment of solids is important as a background in elemental analysis by particle-induced x-ray emission (PIXE)[1]. The variety of physical processes involved in these emissions has stimulated a great deal of interest in recent years. In the present work, the effect of the thickness of the target on the bremsstrahlung yield was determined by the 50 MeV H^o bombardment of aluminum foils of three thicknesses; 0.0025 cm, 0.025 cm, and 0.32 cm. The experimental results are compared with calculations that include bremsstrahlung by the projectile's electron and its cascade, bremsstrahlung by the cascade electrons that are generated by the projectile nucleus and quasifree-electron bremsstrahlung. Relativistic formulae are used. The slowing-down spectra of both the projectile nucleus and the electrons are utilized, as well as the spectrum of cascade electrons. The electron velocity is considered to be isotropic when calculating the angular distribution of the radiation and the spacial distribution of cascade electrons is accounted for in an approximate fashion, as is the loss of electrons through the surface.

II. Experimental Procedures

All of the experiments were carried out on beam line "A" at Argonne National Laboratory using 50 MeV neutral hydrogen. Immediately prior to, and subsequent to, each individual series of experiments the neutral beam was allowed to traverse the specimen chamber, pass through a metal foil sealing the beam line and after traveling a short distance in air, to strike the Faraday cup at the beam stop without interacting with a target. This permitted the fluence of hydrogen atoms striking the target foils to be measured directly. The estimated accuracy of the Faraday cup's determination of the flux in the beam stop is ± 5%. The typical pulse width was approximately 55 microseconds and the current was 20 nanoamps.

The x-ray data were recorded with a liquid nitrogen cooled silicon detector (SiLi) (lithium drifted) made by Princeton Gamma Tech (PGT). Energy calibration of the spectra was obtained by using known standard elements such as: 99.995% aluminum and 99.9995% copper, as well as the $K\alpha_1$ and $K\alpha_2$ lines of tantalum for the low, middle, and upper energy ranges of interest, respectively.

The detector efficiency was calibrated with a Fe^{55} source, produced by Isotope Products Laboratories, which is traceable to the National Bureau of Standards. The calibration was carried out at atmospheric pressure where the absorption due to the air between the source and the detector reduces the signal by a factor of 0.225. This, together with the reduction of 0.994 due to the 0.00033 inch of beryllium detector window, decreases the source's intensity by a factor of 0.224. The source itself experienced an emission rate reduction from its original value of $2.98\text{x}10^6$ to $2.91\text{x}10^6$ photons/second due to radioactive decay over the period of 25 days between the date of its certification and the carrying out of these experiments. Since, the geometric factor comprising area of detector and distance between detector and sample is $5.17\text{x}10^{-5}$ the Fe^{55} source flux at the detector is $(2.91\text{x}10^6)(5.17\text{x}10^{-5})$ $(0.224) = 33.7$ photons per second, which should have produced a flux at the detector of 57,290 photons. The total counts under the experimentally determined spectrum's two iron peaks was 55,448, so that the detector efficiency in the range near 6 keV is calculated to be 96.7%. Comparing this to the efficiency curve supplied by the manufacturer, which is listed at 99.29% at 6 keV, yields an uncertainty in the detector efficiency of about 3%.

The bremsstrahlung radiation produced by 50 MeV neutral hydrogen atoms on the aluminum foils was measured between 3 keV and 23 keV for the 0.0025 cm target; between 3 keV and 28 keV for the 0.025 cm target and between 3 keV and 35 keV for the 0.32 target.

III. Theory

Three mechanisms for continuum x-ray production are significant under the following conditions: (1) The specimen's thickness exceeds the projected range of the incident and secondary electrons; (2) we assume that the velocity of the projectile is large compared with the orbital velocities both of its own electron, and of most of the target's electrons; and, (3) the electrons carried by the ion or atom are stripped from it at a negligible depth in the target. These mechanisms are: electron bremsstrahlung (EB), cascade electron bremsstrahlung (CEB), and quasifree-electron bremsstrahlung (QFEB). The first of these is due to the projectile's electrons, while the other two are caused by its nucleus. These mechanisms are treated separately below.

Although a relativistic formulation is employed, it is assumed that the projectile is not highly relativistic.

We take the projectile ions or atoms to be incident normal to the surface of a plane-bounded solid, and calculate the differential yield of photons escaping the target in the backward hemisphere, i.e., from the surface through which the projectiles enter.

Electron Bremsstrahlung (EB)

The doubly differential yield, $d^2Y/dkd\Omega$, is defined as the number of photons escaping the target with energy k in direction θ, per incident atom, per unit photon energy, per steradian. Then, $d^2Y_{EB}/dkd\Omega$ is the portion of the doubly differential yield that is due to penetration by the electron of the incident atom. Since the angle dependence of the bremsstrahlung differential cross section is not great for speeds that are not highly relativistic, we have ignored the angular dependence of the differential production cross section. In the following approximation, $d^2Y_{EB}/dkd\Omega$ is given, for targets thicker than the projected range of the incident electrons, by the following expression:

$$\frac{d^2Y_{EB}}{dk\, d\Omega} = \frac{N\mathcal{N}}{4\pi\mathcal{I}} \int_0^{\ell} dx\, \exp\left(-\frac{\mu x}{\cos\theta}\right) \int_0^{T_0} dT\, \frac{d^2n}{dxdT}(x,T)\; v\, \frac{d\sigma_t}{dk}(k,T) \quad (1)$$

where $\mathcal{I}$ is the number of atoms striking the target per unit time, $\mathcal{N}$ and T_0 are, respectively, the initial number and initial kinetic energy of electrons in the incident ion or atom, N is the number density of target atoms, ℓ is the target thickness, and $d\sigma_t/dk(k,T)$ is the energy-differential cross section for production of bremsstrahlung of energy k by electrons of kinetic energy T (and velocity v) in collision with target atoms. $d^2n/dxdT$ is the number of electrons in the target at depth x that have kinetic energy T, per unit x per unit T, μ is the absorption coefficient of the solid for photons of energy k and θ is the angle of observation, relative to the outward normal of the back surface of the target. We are concerned in this paper with emission into the backward direction, i.e., through the surface that is exposed to the incident beam, where $\theta < \pi/2$.

It is often the case that the projected range of projectile electrons is less than the extinction length, μ^{-1}, of x rays in the target. By assumption, this range is less than the thickness of the target, as well. Then, a precise description of the range distribution of the electrons is not necessary, and one may replace $d^2n/dxdT$ by $\delta[x-R_{50}(T_0)] \bullet dn/dT$, where $\delta[]$ is the Dirac delta function, and $R_{50}(T_0)$ is the median projected range of electrons with initial energy T_0. Although this is rather a crude approximation, it is useful. The effect upon the yield of the electron range is obtainable, approximately, by comparison with a calculation in which R_{50} is replaced by zero. This effect is seen to be negligible for the most part in the present application, as discussed below.

In the continuous-slowing-down approximation (CSDA), the quantity $\mathcal{J}^{-1}v\,dn/dT$ is given by $S_e(T)^{-1}R(T,T_0)$, where $S_e(T)$ is the stopping power for electrons (energy loss per unit distance traveled) and $R(T,T_0)$ is the ratio of the flux of all electrons (primary plus cascade) of kinetic energy, T, to that of primary electrons alone [2].

Combining the above approximations gives, finally:

$$\frac{d^2Y_{EB}}{dk\,d\Omega} = \frac{NN}{4\pi}\exp\left(-\frac{\mu R_{50}(T_0)}{\cos\theta}\right)\int_k^{T_0} dT\,\frac{R(T,T_0)}{S_e(T)}\,\frac{d\sigma_t}{dk}(k,T) \quad (2)$$

Bremsstrahlung produced by collision of the electron with the target electrons is in principle included in $d\sigma_t/dk$, but the contribution of this process to the yields calculated in the present work is negligible.

Cascade Electron Bremsstrahlung (CEB)

One mechanism of production of continuum x rays by bombardment by swift protons is generation of a cascade of fast electrons, which produce bremsstrahlung in colliding with atoms of the target. The model used here for CEB is similar to the one discussed above for EB. Isotropic emission is assumed, and secondary electrons (arising from proton-target-atom collisions) created at depth x with kinetic energy T_0 are assumed to produce bremsstrahlung at depth $x + R_{50}(T_0)$. The doubly differential yield is given by

$$\frac{d^2Y_{CEB}}{dk\, d\Omega} = \frac{Z_p^{\,2} N}{4\pi} \int_0^{\ell} dx \int_k^{T_{0max}} dT_0 \frac{d\mathcal{N}_s}{dx dT_0} \exp\left(- \frac{\mu(x+R_{50}[T_0])}{\cos\theta}\right)$$

$$\times \int_k^{T_0} dT \frac{R(T.T_0)}{S_e(T)} \frac{d\sigma_t}{dk}(k,T) \qquad (3)$$

where Z_p is the atomic number of the projectile and T_{0max} is the largest value of kinetic energy that is less than or equal to the kinetic limit T_m and satisfies the condition[3] $R_{50}(T_{0max}) \leq \ell - x$. T_m, the maximum energy that can be transferred to a free electron at rest by an ion of velocity v_p, is approximated by $2mv_p^{\,2}/(1-\beta_p^{\,2})$, with $\beta_p = v_p/c$, and m and M are the rest masses of the electron and the projectile nucleus, respectively. $d\mathcal{N}_s/dxdT_0$ is the number of secondary electrons created per target atom at depth x with initial kinetic energy T_0, per unit x per unit T_0, by a projectile nucleus moving in the x direction, and is approximated here by the following extension of a formula given by Fano[4]:

$$\frac{d\mathcal{N}_s}{dxdT_0} = \frac{2\pi Z_p^{\,2} e^4}{mV_p^{\,2}} N \sum_i n_i \left[\frac{1}{(T_0+I_i)^2} - \frac{1-\beta_p^{\,2}}{2mc^2(T_0+I_i)} \right] \quad (4)$$

for $T_0 < T_m$, where n_i and I_i are, respectively, the number of electrons and the ionization potential of the ith shell, in the target atom and v_p is the velocity (taking account of slowing down) at depth x of the projectile.

The above formulation gives a zero yield for photons of energy greater than T_{m0} (the T_m value of the incident ions), where the yield is in reality finite, though falling rapidly with k. This is adequate for the present application, where the measurements do not approach or exceed T_{m0}.

Quasifree-Electron Bremsstrahlung (QFEB)

When an ion's velocity is large compared with that of most of the target electrons, quasifree-electron bremsstrahlung (QFEB)[5,6] is generated. In the frame of the moving ion, the mechanism is bremsstrahlung by the target electrons. The doubly differential yield for this process is given by the following expression:

$$\frac{d^2Y_{QFEB}}{dkd\Omega} = NZ_tZ_p^{\,2} \int_0^{\ell} dx \, \frac{d^2\sigma_p}{dkd\Omega}(k,\theta,v_p) \exp\left(-\frac{\mu x}{\cos\theta}\right) \qquad (5)$$

where Z_t is the atomic number of the target atoms, v_p is the velocity of the projectile nucleus at depth x, taking account of the stopping power and $d^2\sigma_p/dkd\Omega$ is the doubly differential bremsstrahlung production cross section for electron collisions with the projectile nucleus, in a frame in which the electron is initially stationary. This cross section is approximated here by the product of the plane-wave Born approximation expression[6] and the Elwert factor[7], as follows:

$$\frac{d^2\sigma_p}{dkd\Omega} = f_E \frac{\alpha^5}{\pi} Z_t \, Z_p^{\,2} \frac{mc^2}{T_rk} a_o^{\,2} \Bigg[\Bigg[\sin^2\theta + \frac{1}{4}(1+p^2)(3\cos^2\theta - 1) \Bigg\} \Bigg] . \times \ln\left[\frac{1+p}{1-p}\right] - \frac{1}{2} p \, (3\cos^2\theta - 1) \Bigg] \qquad (6)$$

where $p^2 = 1 - k/T_r$, $\alpha \cong 1/137$, a_0 is the Bohr radius, and f_E is the Elwert factor[7], given by

$$f_E = \left[\frac{\nu_2}{\nu_1}\right]\left[\frac{1 - e^{-2\pi\nu_1}}{1 - e^{-2\pi\nu_2}}\right]$$

with $\gamma_1 = Z_p\alpha/\beta_p$ and $\gamma_2 = Z_p\alpha/\beta_2$, where β_2 is the postcollision relative velocity of the projectile nucleus and the electron, divided by c. The cross section goes to zero at $k = T_r$, where T_r is the relative kinetic energy, approximated by m/M times the kinetic energy of the nucleus.

Calculations

Calculated values of the doubly differential bremsstrahlung yield $d^2Y/dkd\Omega$, as well as the separate contributions of the three mechanisms, are shown in Figs 1, 2, and 3 for 50 MeV hydrogen atoms striking aluminum targets at normal incidence, with an angle of observation, θ , of 45^o. Three different target thicknesses are considered. The values of T_{r0} and T_{m0} for 50 MeV protons are 27.2 and 106 keV, respectively. Values of the bremsstrahlung production differential cross section $d\sigma_t/dk$ for electron-aluminum-atom collisions are obtained by fitting to the results of Pratt et al.[8], who treat single-electron transitions in the relativistic self-consistent screened potential of the atom. Values of the median projected electron range R_{50} in aluminum are taken from Lane and Zaffarano[9]. The cascade factor $R(T,T_0) \cong 1 + 0.0221(T_0 /T - 1)^{1.21}$ is obtained by fitting to results of Spencer and Attix[2]. Empirical tabulations are used for the stopping power of aluminum for electrons[10] and for protons[11], and for the absorption coefficient[12] and shell ionization potentials[13].

The doubly differential yield due to the incident electron (and the cascade electrons generated by it), $d^2Y_{EB} /dkd\Omega$, is shown as the dashed curve in Figures 1, 2, and 3. The EB yield goes to zero at $k = T_0 = 27.2$ keV. Note that this contribution to the yield is the same for all three targets. This is because they are all thicker than the median projected range of the projectile electron (treated as a 27.2 keV free electron), $2x10^{-4}$cm.

The yields from the CEB and QFEB mechanisms are given by the dotted-chain and dashed-chain curves, respectively. As shown in Figures 1, 2, and 3, the theory predicts that yields from CEB and from QFEB are of the same order of magnitude, with CEB being the more important mechanism of the two, throughout most of the photon energy range below T_{r0}, the initial value of T_r. This is in agreement with the calculation of Ishii and Morita[14].

The QFEB yield goes to zero at $k = T_{r0}$ (i.e., where k equals the T_r value of the proton at its initial velocity), in the present model. Referring to calculations[15] (done at lower energies) that take account of the electron's motion in the initial state, one expects a finite decrease in the QFEB yield at $k \approx 27$ keV, followed by a tail extending to higher k. Since the predicted QFEB yield is consistently less than the CEB yield, it is considered unlikely that a more precise treatment of the QFEB process would alter the combined yield significantly.

At the lowest proton energies considered, the yields from the CEB and QFEB mechanisms are seen to be practically independent of target thickness. This is because all three targets are thick compared with the photon extinction depth $\mu^{-1} \cos \theta$, which is $3\text{x}10^{-4}$cm at k = 3 keV. However, at higher k (i.e., where $\mu^{-1} \cos \theta$ is greater than target thickness), both the CEB and the QFEB yields increase with thickness, since these targets are range-thin for the 50 MeV proton.

Eqs. (2) and (3) for $d^2Y_{EB}/dkd\Omega$ and $d^2Y_{CEB}/dkd\Omega$ contain $R_{50}(T_0)$ as a simple way to take account of the effects of electron ranges on the x-ray yields, as discussed above. These effects, which reduce the x-ray yields, are probably exaggerated in those equations. In order to estimate the magnitudes of these effects (and hence the possible error), calculated yields are compared with a second set of computations, in which R_{50} is replaced by zero. In the EB process, when R_{50} is included, the yield is reduced at the lowest k values (by 24% at k = 3 keV and 7% at 5 keV), but is reduced by less than 1% for k > 10 keV. In the CEB mechanism, the factor exp $(-\mu R_{50}/\cos \theta)$ in Eq. (3) leads to a reduction of the yield at small k (by 54% at k = 3 keV, 30% at 5 keV, 7% at 10 keV, and 1.5% at 20 keV). In addition, there is the dependence[3] of T_{0max} on R_{50}. This has less than a 1% effect on the 0.32 cm target and less than 6% on the 0.025 cm target, but becomes significant for the 0.0025 cm target, where the reduction is negligible at k = 3 keV, but rises slowly to 40% at 20 keV, 60% at 50 keV and 70% at 70 keV. As far as the total yield, $d^2Y/dkd\Omega$, is concerned, the errors introduced in the present calculations by the approximate treatment of electron range are probably well below 10%, for photon energies above 4 keV, except for the yield of k > 20 keV photons from the 0.0025 cm target.

IV. Experimental Results

Figure 4 compares the experimentally determined bremsstrahlung yields from the 0.0025 cm, 0.025 cm, and 0.32 cm aluminum foils, with the theoretical predicted total yields for these thicknesses. It is seen that at 20 keV, for example, there is almost an order of magnitude change in the experimentally determined bremsstrahlung yield corresponding to the almost order of magnitude change in the foil thicknesses. This is due to the sharp differences in slope of the yield versus photon energy curves as a function of foil thickness. The sharp peaks which appear on each of the experimental curves are due to characteristic $K\alpha$ x-ray lines and to a γ line. The characteristic lines are due to the beam scattering from the target foils and striking the walls of the stainless steel test chamber. Chromium, iron, cobalt, and nickel $K\alpha$ lines can be seen at 5.4 keV, 6.4 keV, 6.9 keV, and 7.5 keV, respectively. The γ line at 14.4 keV is due to the reaction: $^{56}Fe^{30} + {}^{1}p^{0}$ $^{57}Co^{30}$ + 14.4 keV[16].

V. Discussion

A comparison of the theoretically predicted bremsstrahlung yields with experimentally determined values is shown in Figure 4. It can be seen that the agreement is relatively good and that the shape of the theoretical curves, their slopes, and their quantitative yields are very close to the experimental curves for all three thicknesses of aluminum targets. The experimental yields are larger than the theoretical values by factors which range between 2 and 3, with the error increasing with foil thickness but decreasing, somewhat, with photon energy. A review of the potential errors introduced by assumptions made in developing the theoretical yields cannot account for differences of factors of 2 or 3.

The terms used in the equations for $d^2Y_{EB}/dkd\Omega$, $d^2Y_{CEB}/dkd\Omega$, and $d^2Y_{QFEB}/dkd\Omega$ were obtained from experimental data or empirical tables. This includes values for the bremsstrahlung production differential cross-sections, $d\sigma/dk$, the cascade factor $R(T,To)$, the stopping power of aluminum for electrons and protons, the absorption coefficient, and the shell ionization potentials. Consequently, it is difficult to conclude that the errors introduced by the assumptions used inn the calculation of the total yield can be as large as factors of 2 to 3 which would be required in order to accommodate the difference shown in Figure 4 between the theoretical and experimental curves.

However, in considering the details of the experimentally determined yields, there is a phenomenon which could have contributed to values larger than the theoretically determined ones. Figure 4 clearly shows characteristic $K\alpha$ x-ray lines superimposed on top of the general bremsstrahlung background. These lines are produced by primary and secondary particles and energetic photons scattering from the foils and striking the specimen holder and the walls of the stainless steel test chamber, some of which enter the detector. Moreover, the scattered beam will strike the target foils again, producing additional bremsstrahlung radiation. It is noted in Figure 4, that the difference between the experimental curves and the theoretical curves increases with thickness. This would be consistent with the suggestion that thicker targets produce more divergence of the beam and thus more "extraneous" bremsstrahlung radiation from the walls of the chamber. Further support for this suggestion comes from noting that the intensity of the 14 keV gamma peak increases by almost an order of magnitude as the thickness of the target increases from 0.0025 cm to 0.32 cm. While a quantitative analyses has not been carried out to determine the extent of this experimentally produced "extraneous" Bremsstrahlung, a factor of 2 to 3 above the theoretically predicted value does not seem extreme.

Acknowledgments

This research was supported jointly by the SDIO LTH-4 program and under DNA Task Code X99QMXXD and Work Unit Code 00003, sponsored by the Weapons Laboratory, under Interagency Agreement DOE No. 1418-1418-A1 and the Office of Health and Environmental Research, U.S. Department of Energy, under Contract DE-AC05-840R21400 with Martin Marietta Energy Systems, Inc. The authors gratefully thank the Argonne National Laboratory's staff who operated the Neutral Particle Beam Test Stand for their assistance in providing us with energetic atoms and D.A. Cushing and S.S. McCready of the Air Force Weapons Laboratory for their computer code assistance.

References

1. F.Folkmann, C.Gaarde, T.Huus and K.Kemp, Nucl. Instr. Meths. 116, 487 (1974).
2. L.V.Spencer and F.H.Attix, Rad. Res. 3, 239 (1955).
3. Secondary electrons are assumed to escape without producing radiation, if and only if, they are born at a depth greater than $\ell - RP_{50}(T_0)$, where T_0 is their initial kinetic energy.
4. U.Fano, in "Studies in Penetration of Charged Particles in Matter", Committee on Nucl. Sci., Nucl. Sci. Series Rept. No. 39, P.287, (Nat. Acad. of Sci.-Nat. Research Council Publication 1133, Washington D.C., 1964).
5. H.W.Schnopper, J.P.Delvaille, K.Kalata, A.R.Sohval, M.Abdulwahab, K.W.Jones and H.E. Wegner, Phys. Lett. 47A, 61 (1974).

6. A.Yamadera, K.Ishii, K.Sera, M.Sebata and S.Morita, Phys. Rev. A 23, 24 (1981).
7. G.Elwert, Ann. Phys. 34, 178 (1939).
8. R.H.Pratt. H.K.Tseng, C.M.Lee, L.Kissel, C.MacCallum, and M.Riley, At. Data and Nucl. Data Tables 20, 175 (1977).
9. R.O.Lane and D.J.Zaffarano, Phys. Rev. 94, 960 (1954).
10. Internat. Commission on Radn. Units and Measurements, *Stopping Powers for Electrons and Positrons*, ICRU Report 37 (ICRU, Bethesda MD) 76, 6 (1984).
11. J.F.Ziegler, *Handbook of Stopping Cross Sections for Energetic Ions in All Elements*. Vol. 5 of *The Stopping and Ranges of Ions in Matter*, Ed. by J.F.Ziegler (Pergamon, New York, 1980), p. 141.
12. H.J.Hagemann, W.Gudat and C.Kunz, DESY Report SR-74/7 (1974).
13. H.A.Bearden and A.F.Burr, Revs. Mod. Phys. 39, 125 (1967).
14. K.Ishii and S.Morita, Nucl. Instr. Meths. B3, 57 (1984).
15. K.Ishii and S.Morita, Phys. Rev. A 30, 2278 (1984).
16. E.Browne, J.M.Dairiki, R.E.Doebler, A.A.Shihab-Eldin, L.J.Jardine, J.K.Tuli and A.B.Buyrn, *Table of Isotopes Seventh Edition*, Ed. by C.M.Lederer and V.S.Shirley (John Wiley & Sons, Inc., New York, 1978), p.165.

Figures

Figure 1. Calculated values of double differential Bremsstrahlung yield from a 0.0025 cm thick Al target bombarded with 50 MeV H^{o} atoms observed at 45^{o}.

Figure 2. Calculated values of doubly differential Bremsstrahlung yield from a 0.025 cm thick Al target bombarded with 50 MeV H^{o} atoms observed at 45^{o}.

Figure 3. Calculated values of doubly differential Bremsstrahlung yield from a 0.32 cm thick Al target bombarded with 50 MeV H^{o} atoms observed at 45^{o}.

Figure 4. Comparison of experimental and theoretical results of doubly differential Bremsstrahlung yields, $d^2Y/dkd\Omega$, from three different thicknesses of Al bombarded with 50 MeV H^{o} atoms observed at 45^{o}.

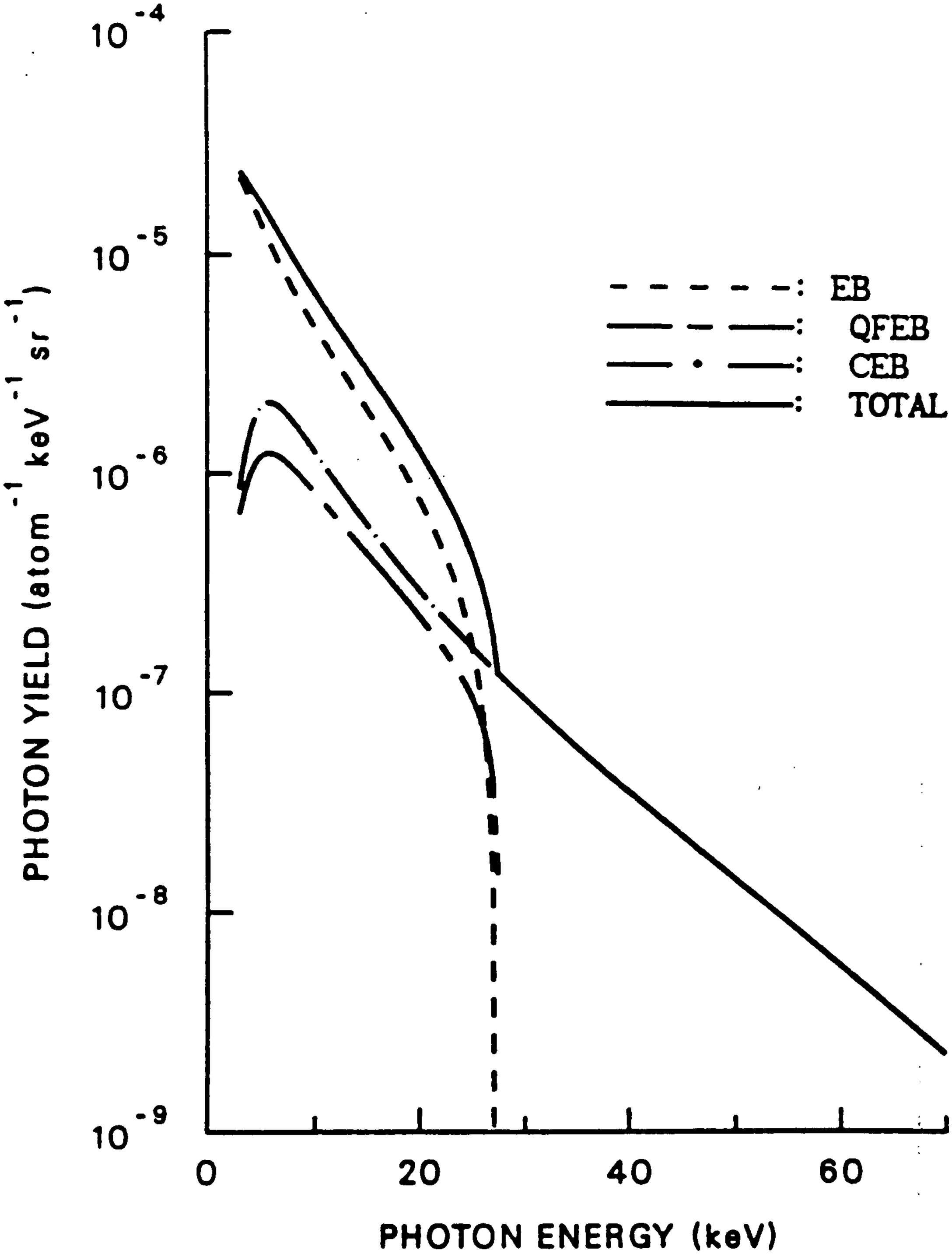

10^{-4}
10^{-5}
10^{-6}
10^{-7}
10^{-8}
10^{-9}
PHOTON YIELD (atom^{-1} keV^{-1} sr^{-1})
0
20
40
60
PHOTON ENERGY (keV)
EB
QFEB
CEB
TOTAL

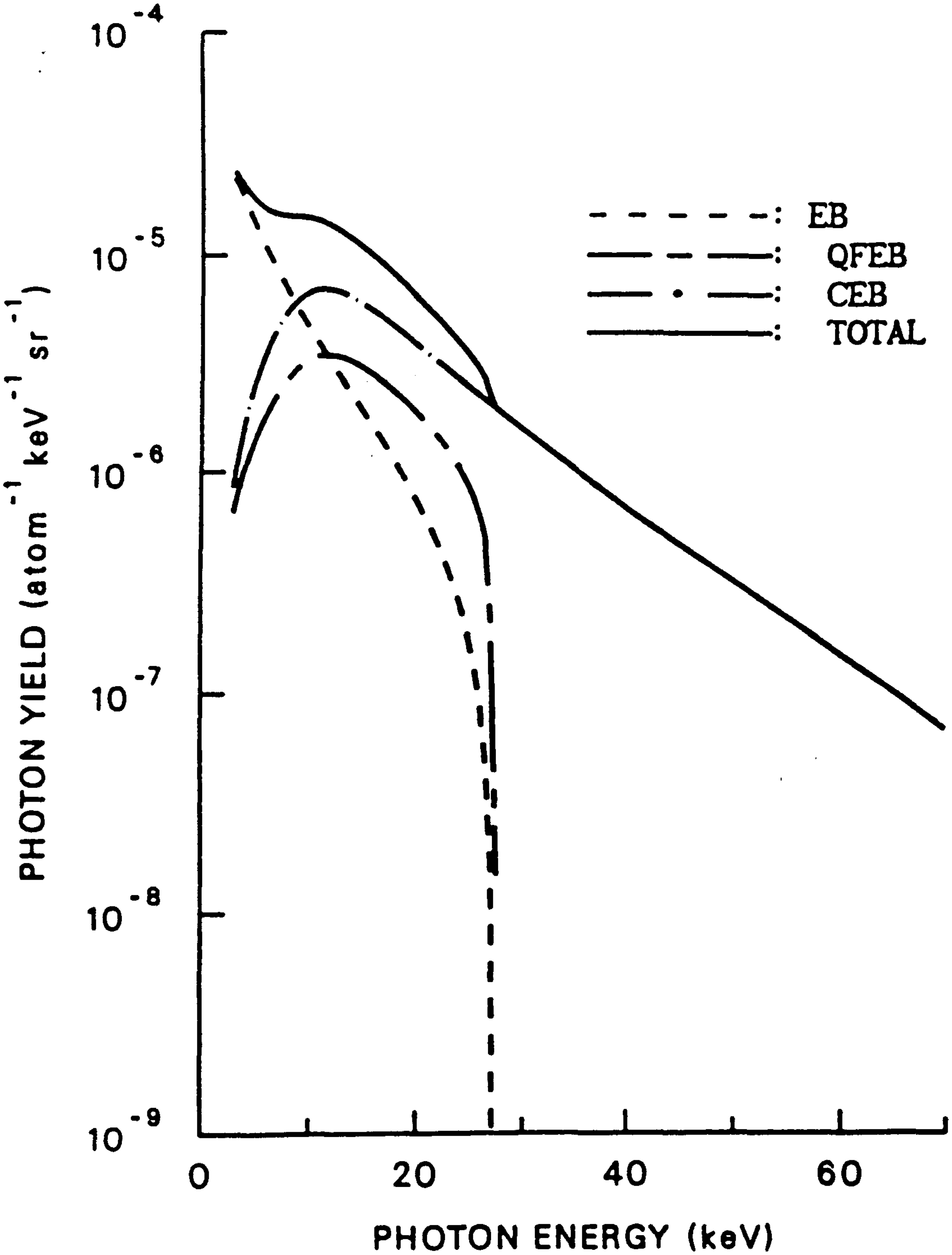
PHOTON YIELD (atom^{-1} keV^{-1} sr^{-1})
10^{-4}
10^{-5}
10^{-6}
10^{-7}
10^{-8}
10^{-9}
0
20
40
60
PHOTON ENERGY (keV)
- - - - - -: EB
——— — ———: QFEB
——— • ———: CEB
————————: TOTAL

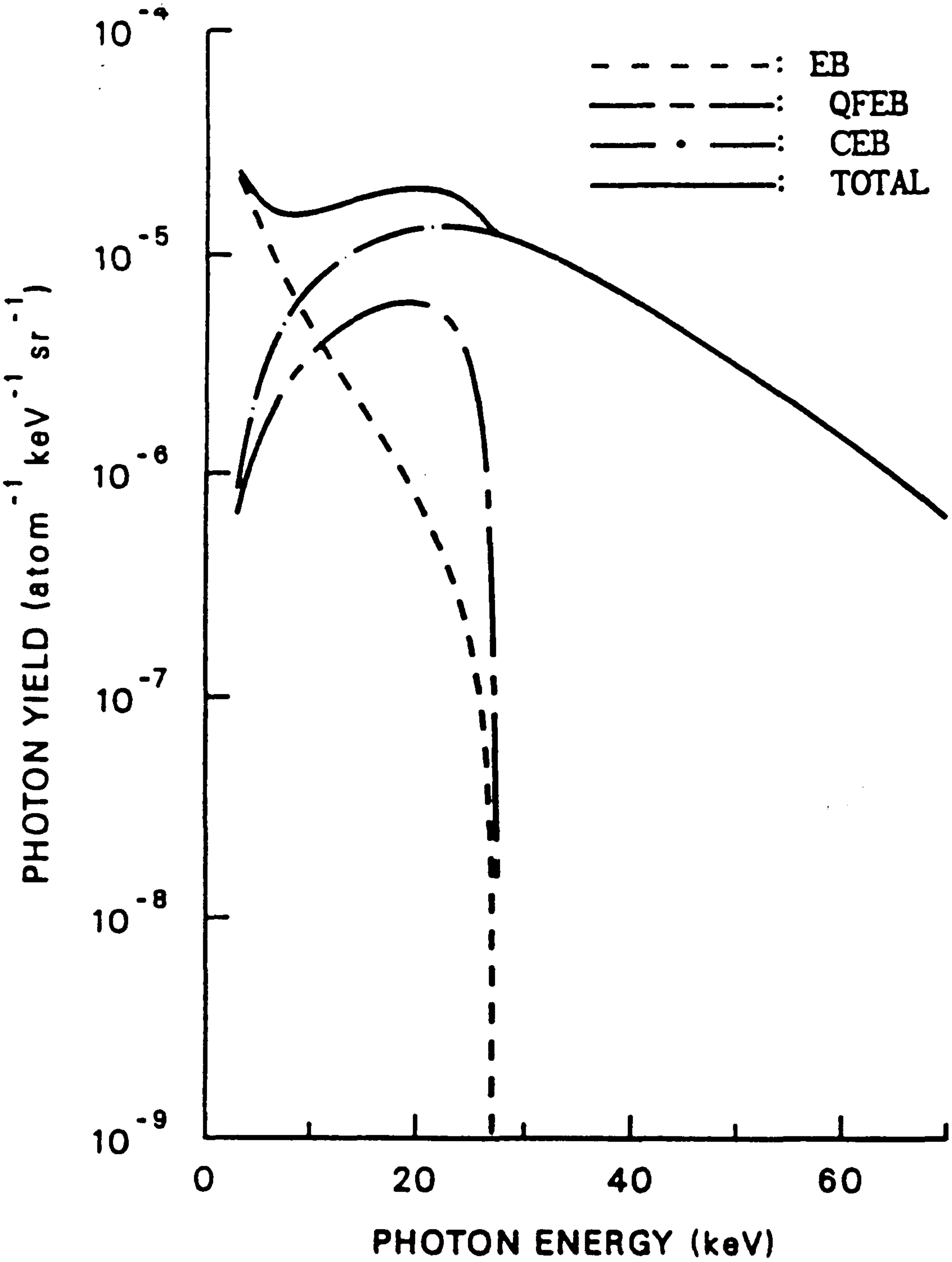

- - - - - -: EB
—— — — ——: QFEB
—— • ——: CEB
————: TOTAL
10^{-4}
10^{-5}
10^{-6}
10^{-7}
10^{-8}
10^{-9}
PHOTON YIELD (atom^{-1} keV^{-1} sr^{-1})
0
20
40
60
PHOTON ENERGY (keV)

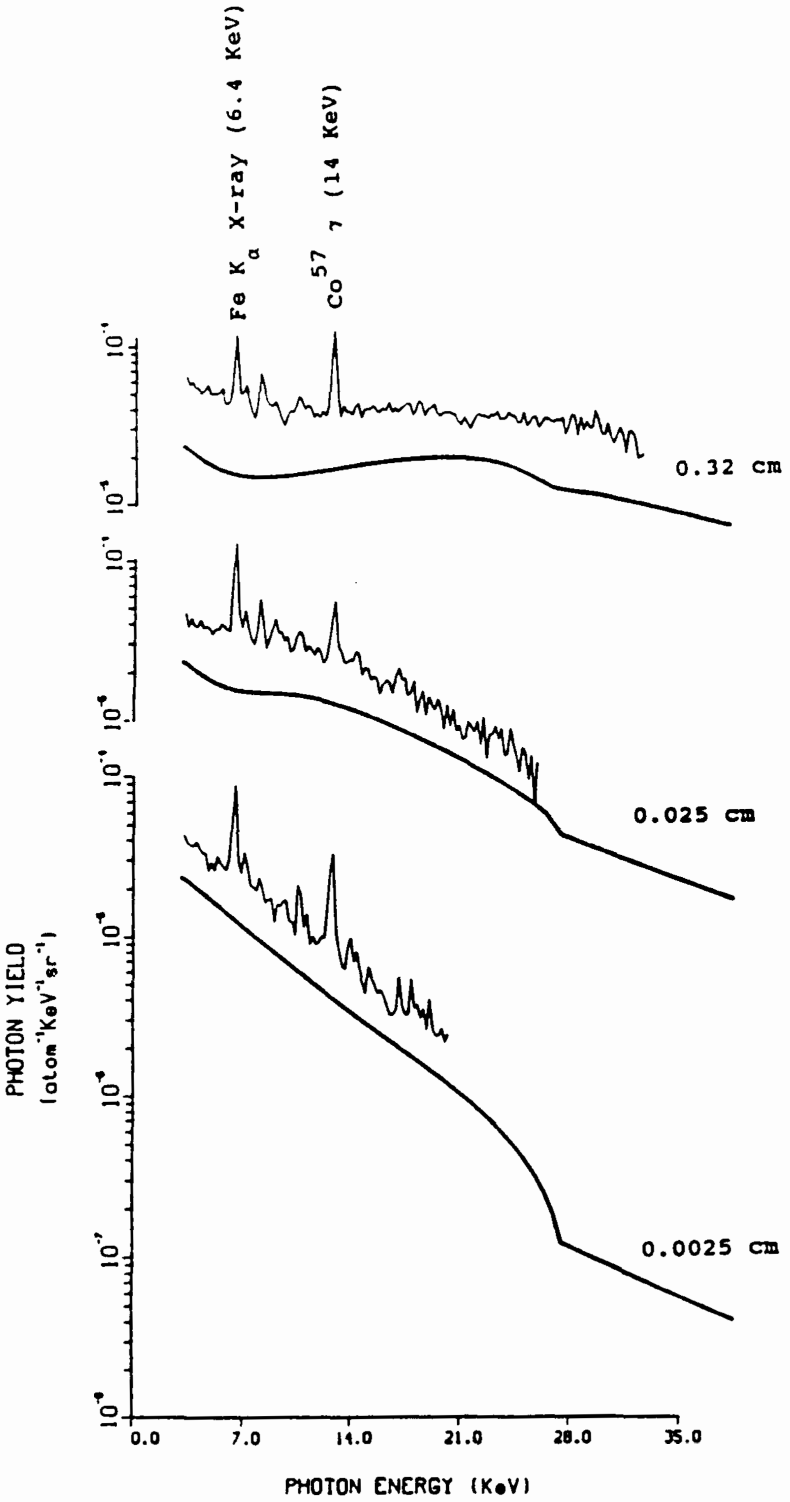

Fe K$_\alpha$ X-ray (6.4 KeV)
Co^{57} γ (14 KeV)
0.32 cm
0.025 cm
0.0025 cm
PHOTON YIELD
(atom^{-1}KeV^{-1}sr^{-1})
10^{-4}
10^{-5}
10^{-4}
10^{-5}
10^{-4}
10^{-5}
10^{-6}
10^{-7}
10^{-8}
0.0
7.0
14.0
21.0
28.0
35.0
PHOTON ENERGY (KeV)